Self-assembled CaF_2 nanostructures on silicon

D. Y. Petrovykh,[a] J. Viernow,[b] J.-L. Lin, F. M. Leibsle,[c] F. K. Men,[d] A. Kirakosian, and F. J. Himpsel[e]
Department of Physics, University of Wisconsin Madison, Madison, Wisconsin 53706-1390

(Received 9 October 1998; accepted 22 February 1999)

A method for chemical imaging of CaF_2, CaF_1, and Si by scanning tunneling spectroscopy is presented. This method is utilized for identifying the growth regimes of CaF_2 and CaF_1 on stepped Si(111)7×7. For CaF_2 on Si(111), we find random islands, stripes, and ordered islands, depending on the supersaturation. For CaF_2 on a CaF_1 monolayer on Si(111), we find regular stripes that are continuous and separated from each other. CaF_2 structures are attached to the bottom edge of a step when growing directly on Si, but they prefer the top of a step edge when growing on a CaF_1 buffer layer. These highly regular, linear arrays of CaF_2 stripes and dots can serve as masks for assembling more sophisticated nanostructures. © *1999 American Vacuum Society.* [S0734-2101(99)12204-8]

I. INTRODUCTION

The growth of CaF_2 on Si(111) has been studied extensively[1–13] because this combination is lattice matched and grows epitaxially. That opens possibilities for epitaxial metal–insulator–semiconductor (MIS) devices and, eventually, to truly three-dimensional semiconductor devices. Many studies have focused on the structure and electronic states of the CaF_2/Si(111) interface which is crucial to the functioning of MIS field effect transistors (FET's). Two types of interfaces have been found, a F-terminated interface at temperatures below 700 °C, and a Ca-terminated interface from 700 °C to the desorption of CaF_2 at 800 °C (for a monolayer). The F-terminated interface has a large band gap comparable to that of bulk CaF_2 (12 eV), which is reduced to 2.4 eV at the Ca-terminated interface,[11] due to an extra electron in the Ca 4*s* orbital. The F-terminated interface preserves the orientation of the Si(111) substrate (type A epitaxy), while the Ca-terminated interface rotates the structure azimuthally by 180° (type B epitaxy).[1–4]

Steps are capable of influencing the growth mode of CaF_2 in several ways. Because of the 180° rotation of the Ca-terminated interface,[1] a CaF_1 film growing on a lower terrace is mismatched with the Si on the adjacent upper terrace. Another effect has been found by Si 2*p* core level spectroscopy:[5] A significant fraction of the interface remains F-terminated on a stepped surface, even at high annealing temperatures where the Ca-terminated structure is found on flat Si(111). Furthermore, a significant influence of steps has been inferred in detailed work on the temperature- and rate-dependent growth modes.[7] In general, one would expect a transition from island nucleation to step flow growth with decreasing supersaturation, that is, increasing temperature, decreasing rate, and decreasing step spacing. As soon as CaF_2 molecules are able to diffuse to the nearest step edge they become attached to it. Our goal is to observe the microscopic basis of these phenomena by using scanning tunneling microscopy (STM).

II. CHEMICALLY SENSITIVE STM

Distinguishing between CaF_2, CaF_1, and Si substrate can become quite difficult for the complex surface topography that can result from growth at stepped surfaces. To solve this problem, we have tested various spectroscopic imaging methods, such as resonant tunneling,[14] and have found a new, ''antiresonant'' tunneling method to be very useful.[15] CaF_2 and Si do not have sharp resonances that could be used for chemically-specific tunneling. However, CaF_2 exhibits a large, 12 eV band gap which suppresses the tunneling current greatly for bias voltages within the gap. That gives CaF_2 patches on the surface a dark appearance in current images taken at a bias voltage within the gap. The approach is illustrated in Fig. 1 by images of the growth pattern of islands of CaF_2 on a stepped Si(111)7×7 surface. The resolution of this chemical imaging method is at the 1 nm level or better (Fig. 1, bottom).

In practice, we stabilize the tunneling current (0.3–1.0 nA) at a sample bias voltage of +4 V, where electrons from the tip tunnel into the conduction band minimum[13] (CBM) of CaF_2. Figure 1 (top) presents a topographic image obtained in this fashion. Sufficient sample bias voltage is essential for tunneling into insulators in general. Any attempts to stabilize the tunneling current at bias voltages below the conduction band minimum result in a tip crash, because the insulating layer acts like vacuum, thereby forcing the tip to approach the underlying Si in search of a tunneling current.

For obtaining the chemical image in Fig. 1 (center), a simultaneous current image is acquired at a bias voltage of +2 V, i.e., inside the gap of CaF_2. The topography is simplified in this image, e.g., the height difference between Si terraces is eliminated. Only the chemical composition of the surface determines the contrast, with CaF_2 dark and Si

[a]Electronic mail: dypetrov@students.wisc.edu
[b]Permanent address: Institut für Festkörperphysik, Universität Hannover, D-30167 Hannover, Germany.
[c]Permanent address: Department of Physics, University of Missouri, Kansas City, Kansas City, MO 64110.
[d]Permanent address: Department of Physics, National Chung Cheng University, Taiwan, R.O.C.
[e]Electronic mail: himpsel@comb.physics.wisc.edu

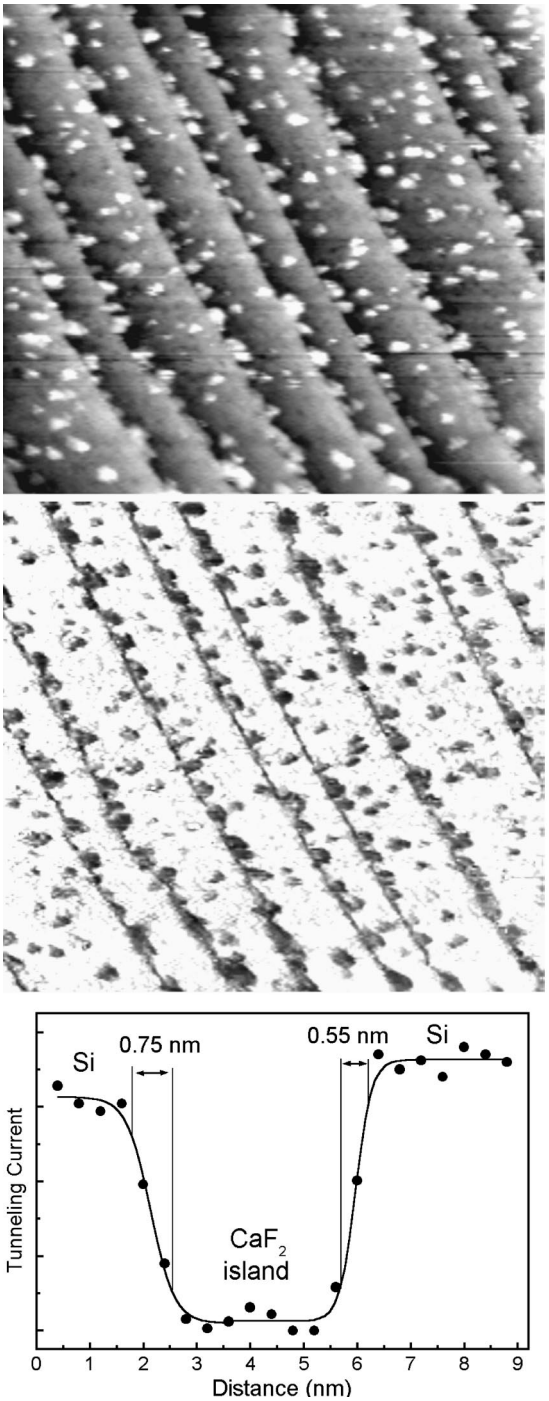

FIG. 1. Chemical imaging of small CaF_2 islands on Si(111)7×7. 100×80 nm^2. Top: Topography obtained at a sample bias of +4 V with a tunneling current of 1 nA, exhibiting Si steps with small islands of adsorbed CaF_2. Center: Chemical image, obtained from the tunneling current distribution at a sample bias of +2 V, while stabilizing the tip height at a sample bias of +4 V. Electrons from the tip cannot enter the gap of CaF_2, resulting in a low current for CaF_2 patches (dark areas). Height difference between terraces is eliminated and the contrast is reversed, with Si appearing bright and CaF_2 dark. Bottom: Line scan across a CaF_2 island demonstrating a resolution of better than 1 nm. This resolution limit corresponds to the change in the tunneling current from 85% to 15% of the maximum value.

bright. For CaF_2 islands on a Si substrate, the assignment of different features is not very ambiguous. However, in case of a more complicated surface structure, such as bunched Si steps, step flow, and step etching, the difference between the

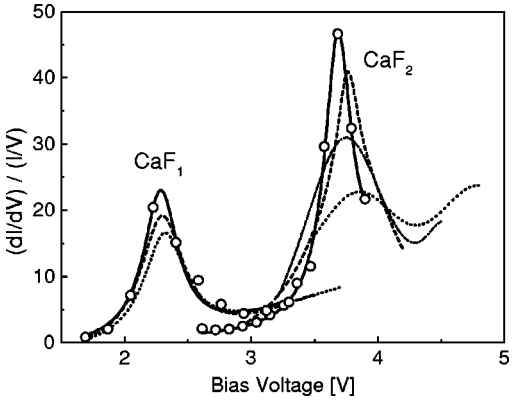

FIG. 2. Scanning tunneling spectra of CaF_1 and CaF_2 showing the onset of the conduction band minimum at different voltages. Different line types represent different tip heights.

substrate and the adsorbate is not always apparent in the topography image. The current image also allows identification of the chemical state (CaF_2 vs CaF_1) due to the difference in band gap (more on that in Fig. 2).

It is well known that a mixture of topographic and chemical contrast is seen in the topography mode. For example, at a sample bias of +4 V (Fig. 3) the CaF_2 islands and stripes appear higher (brighter) than equivalent Si terraces, even though CaF_2 is lattice matched to Si within <1%. There must be enhanced tunneling into states near the conduction band minimum of CaF_2, which is further supported by the resonance in the tunneling spectra at a bias voltage close to the CBM (Fig. 2).

The spectroscopic underpinnings of our chemical imaging method are shown in Fig. 2. Essentially, we take advantage of an unexpectedly large jump in the conductivity at the conduction band minimum of insulators, which allows us to use the energy of the CBM relative to the Fermi level as the chemical identifier. The differential conductance (dI/dV) or its normalized version $(dI/dV)/(I/V)$ can be obtained from the scanning tunneling spectroscopy $I(V)$ curves. The conduction band edges correspond to onsets in the (dI/dV) curves and become well-defined peaks in the normalized spectra (Fig. 2). While the exact origin of such strong and narrow peaks is still being investigated,[15] it is interesting to note that the 3.7 eV peak in Fig. 2 for CaF_2 is consistent with the 3.6–3.8 eV CBM position expected from macroscopic observation techniques,[5,6] but the 2.3 eV CaF_1 peak is higher than the expected[11] 1.4–1.8 eV.

III. GROWTH MODES AT STEPS

General growth models[7,16] predict a transition from island nucleation to step flow growth with increasing temperature, decreasing rate, and decreasing step spacing. Growth in general is a nonequilibrium process for which a particular outcome is determined by the combined influence of these parameters, together with the total coverage. The growth

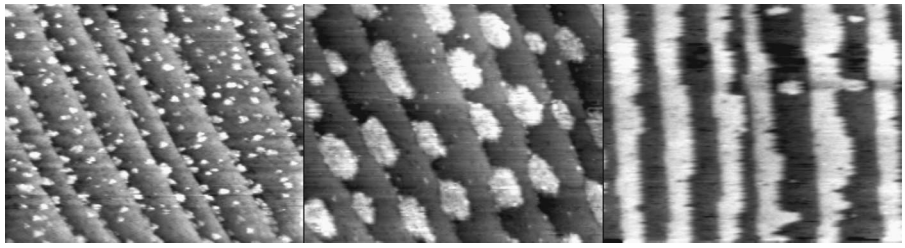

FIG. 3. Three growth regimes for CaF_2 on Si(111)7×7 with single steps, tilted 1.1° towards $(\bar{1}\,\bar{1}\,2)$. Downhill is to the right. CaF_2 appears bright. 100×80 nm^2. Left: Island growth at 550 °C (compare Fig. 1). The island size (≈2 nm) decreases at lower temperature in proportion to the shrinking diffusion length. Center: Strings of regular islands (10 nm) attached to the Si step edges. These are formed at higher mobility and deposition rate (growth at 650 °C and post-annealed at 700 °C for 5 min). Right: Step flow growth at 600 °C, producing CaF_2 stripes 5–10 nm wide.

modes studied for CaF_2 in this work can be classified according to the respective temperature-rate-coverage combinations:

(1) Low temperature[17] (550 °C), low deposition rate, and low coverage result in randomly distributed small islands (Fig. 3, left). The average size and separation are determined by the CaF_2 diffusion length.

(2) Increasing temperature (650 °C) and deposition rate, together with a low coverage result in strings of CaF_2 ''dots'' attached to the Si step edges (Fig. 3, center). Under these conditions, CaF_2 molecules are able to diffuse towards the preferred sites adjacent to Si steps and form larger dots. The dot size and spacing appear to be self-limited,[18] leading to uniform structures.

(3) Moderate increase of temperature (600 °C) and coverage, combined with lower deposition rate result in typical step-flow growth (Fig. 3, right).

(4) Substantial increase in temperature (700 °C and above) leads to desorption processes. On larger terraces, a conversion of CaF_2 to CaF_1 interface is observed. On narrow terraces, we find that CaF_2 desorbs by etching away Si step edges, leading to Si step edges receding between remaining CaF_2 stripes and dots. A likely reaction is the formation of volatile SiF_4 plus a remaining Ca layer on Si, which we see as single-domain 3×1 structure.[19]

(5) Moderate temperature (610–630 °C) combined with a coverage between 1 and 2 monolayers lead to a qualitatively different growth mode where highly perfect CaF_2 stripes are formed on top of a CaF_1 monolayer (Fig. 4, top).

At the lowest growth temperatures, islands nucleate spontaneously and ripen by sweeping up CaF_2 molecules that land within a diffusion length of an island. Consequently, the size of the islands and their average spacings are related to the diffusion length.[16] For growth at 550 °C and 5 s (Fig. 3, left), we find an average island diameter of about 2 nm, for growth at 650 °C and 10 s, the average island diameter is about 10 nm. Islands are noticeably absent in the region adjacent to the upper edge of a step. A systematic analysis of images taken in the island growth regime at 550 °C verifies this observation. It suggests that CaF_2 is bound less strongly at the upper edge of a step.

At higher temperatures and faster deposition, CaF_2 forms a regular array of islands attached to the step edges. In Fig. 3 (center) the coverage is 1/5 of a monolayer of CaF_2 deposited at 650 °C with a brief postanneal at 700 °C. This growth mode is reminiscent of the Stranski–Krastanov growth in two dimensions, except that the CaF_2 islands are much more regular.[20] A competition between ripening into large dots and an upper size limit imposed by misfit strain may be responsible for size homogeneity. High deposition rate and

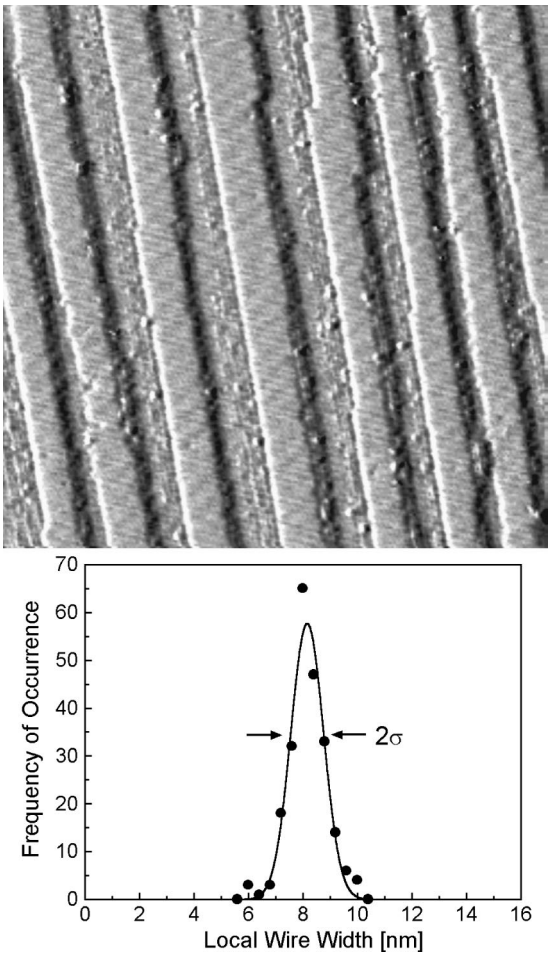

FIG. 4. CaF_2 stripes grown on a Si(111) surface coated by CaF_1. Top: STM image, showing the *x* derivative of the tip height, simulating illumination from the left. Note that the CaF_2 stripes are attached to the top of the step edges. Downhill is to the right. 100×100 nm^2. Bottom: Width distribution along one of the stripes in Fig. 4 top.

increased mobility of CaF_2 at this elevated temperature lead to a supersaturation nucleation and growth when the formation of new nucleation sites is suppressed after a critical island concentration is attached. Nucleation at step edges is preferred due to the higher coordination of such sites.

The Si step separation of 15 nm and the dots sizes of 7×10 nm in growth mode 2 lead to arrays of dots that may be used as precursors for creating ultradense storage media. Their density is on the scale of 10^{11} dots/cm^2, or Teradots per square inch, in units commonly used in the storage industry. This represents a thousand-fold increase compared to commercially available densities of few Gigabits per square inch in hard disks. The linear arrangement of the islands along the straight step edges makes this growth mode particularly suited for possible linear readout architectures, such as shift registers or scanning probes and reading heads.

The main difference between modes shown in Fig. 3 center and right is that in the latter case deposition rate is lower which combined with considerable mobility of CaF_2 molecules at 600 °C gives rise to the step flow growth mode. Higher coverage allows the formation of CaF_2 stripes which decorate the Si(111) step edges (Fig. 3, right). For growth at 600 °C in 10 s and half a monolayer coverage, we find that on the terraces narrower than 17 nm all the CaF_2 has been swept into the stripes at the step edge. Given approximately half-monolayer coverage molecules had to diffuse at least across half the terrace (8–9 nm) to become attached. The first islands remaining on the clean part of terraces appear for terrace widths of about 20–25 nm, suggesting that CaF_2 molecules could not diffuse farther than 10–12 nm. The two observations combined lead to a diffusion length of the order of 10 nm at these growth conditions.

Figure 4 (top) presents an example of a more complicated growth mode. After depositing 1.5 monolayers of CaF_2 at 610–630 °C and a postanneal to 830 °C for 30 s, a complete overcoat of CaF_1 is established with CaF_2 stripes on top of it. Chemical imaging confirms the identity of the two species. Unlike the CaF_2 on Si stripes and dots described above, the stripes grown on CaF_1 are formed exclusively on the top edges of Si steps.[20] In fact they avoid the bottom edge to such extent, that even for coverage very close to 2 monolayers, there is always an uninterrupted CaF_1 gap between a stripe and a bottom edge of a Si step. A simple explanation for this strikingly different behavior comes from the fact that the Ca-terminated interface (i.e., CaF_1 layer underneath CaF_2) rotates the lattice by 180° around the normal.[4] The CaF_2 stripes are then laterally mismatched with the adjacent Si step and avoid it. Position on top of the step on the other hand allows CaF_2 to maintain its preferred orientation. Note that the F-terminated interface does not induce such a 180° rotation,[4] so the CaF_2 structures grown at lower temperature and coverage are matched with the adjacent Si steps and preferentially grow attached to their bottom edges (Fig. 3).

The interaction described above leads to formation of continuous and completely separated CaF_2 stripes[20] (Fig. 4, top) and also helps to keep them rather homogeneous. With the help of a pattern recognition algorithm we can quantify the width distribution along a single stripe. The resulting distribution is presented in Fig. 4 (bottom). A simple Gaussian fit (solid curve) gives a mean width of 8 with 0.6 nm standard deviation. Such homogeneous and continuous stripes can serve as templates for selective deposition of insulated metallic nanowires with widths in the single digit nanometer range. Some possible chemically selective deposition processes are being currently investigated.[21]

IV. SUMMARY AND OUTLOOK

In summary, we have developed a chemical imaging method for STM, using antiresonant tunneling into the band gap of insulating CaF_2. This technique should be generally applicable to the chemical imaging of insulators with different band gap by STM. Using it for determining the microscopic growth mode of CaF_2 on stepped Si(111)7×7, we have found interesting effects, such as CaF_2 stripes in the step flow regime, regular CaF_2 island arrays at low coverage and high supersaturation, the repulsion of CaF_2 on Si from the upper step edge, and repulsion of CaF_2 on CaF_1 from the lower step edge induced by the Ca-terminated interface lattice rotation.

A longer range goal of this work is establishing universal methods for nanolithography or wires by self-assembly at step edges.[22] It is already possible to produce highly perfect step arrays[23] on Si(111)7×7. Stripes and dots of CaF_2 attached to Si step edges should be able to play a role similar to the photoresist in ordinary microlithography, passivating the underlying Si. That would provide the essential ingredients for controlled nanolithography of wires and dots.

ACKNOWLEDGMENTS

This work was supported by NSF under Award Nos. DMR-9624753 and DMR-9632527.

[1]T. Asano and H. Ishiwara, Appl. Phys. Lett. **42**, 517 (1983); C.-C. Cho, H. Y. Liu, B. E. Gnade, T. S. Kim, and Y. Nishioka, J. Vac. Sci. Technol. A **10**, 769 (1992).
[2]T. P. Smith III, J. M. Phillips, R. People, J. M. Gibson, L. Pfeiffer, and P. J. Stiles, Mater. Res. Soc. Symp. Proc. **54**, 295 (1986).
[3]C.-C. Cho, T. S. Kim, B. E. Gnade, H. Y. Liu, and Y. Nishioka, Appl. Phys. Lett. **60**, 338 (1992).
[4]R. M. Tromp and M. C. Reuter, Phys. Rev. Lett. **61**, 1756 (1988); **73**, 110 (1994).
[5]F. J. Himpsel, F. U. Hillebrecht, G. Hughes, J. L. Jordan, U. O. Karlsson, F. R. McFeely, J. F. Morar, and D. Rieger, Appl. Phys. Lett. **48**, 596 (1986); D. Rieger, F. J. Himpsel, U. O. Karlsson, F. R. McFeely, J. F. Morar, and J. A. Yarmoff, Phys. Rev. B **34**, 7295 (1986); F. J. Himpsel, U. O. Karlsson, F. R. McFeely, J. F. Morar, D. Rieger, A. Taleb-Ibrahimi, and J. A. Yarmoff, Mater. Sci. Eng., B **1**, 9 (1988).
[6]M. A. Olmstead, R. I. G. Uhrberg, R. D. Bringans, and R. Z. Bachrach, Phys. Rev. B **35**, 7526 (1987).
[7]J. D. Denlinger, E. Rotenberg, U. Hessinger, M. Leskovar, and M. A. Olmstead, Phys. Rev. B **51**, 5352 (1995); U. Hessinger, M. Leskovar, and M. A. Olmstead, Phys. Rev. Lett. **75**, 2380 (1995).
[8]Ph. Avouris and R. Wolkow, Appl. Phys. Lett. **55**, 1074 (1989).
[9]M. T. Cuberes, A. Bauer, H. J. Wen, M. Prietsch, and G. Kaindl, J. Vac. Sci. Technol. B **12**, 2646 (1994).
[10]T. Nakayama, M. Katayama, G. Selva, and M. Aono, Phys. Rev. Lett. **72**, 1718 (1994).
[11]T. F. Heinz, F. J. Himpsel, E. Palange, and E. Burstein, Phys. Rev. Lett. **63**, 644 (1989); F. J. Himpsel, T. F. Heinz, A. B. McLean, E. Palange, and E. Burstein, J. Vac. Sci. Technol. B **7**, 879 (1989).

[12]H. Fujitani and S. Asano, Phys. Rev. B **40**, 8357 (1989); Surf. Sci. **268**, 265 (1992); M. R. Salehpour, S. Satpathy, and G. P. Das, Phys. Rev. B **44**, 8880 (1991); S. Ossicini, A. Archangeli, and O. Bisi, *ibid*. **43**, 9823 (1991); Surf. Sci. **269/270**, 743 (1992).

[13]Typical band offsets between the conduction band minimum of CaF_2 and that of Si(111) are between 2.5 and 4 eV (see Refs. 5,6). The Fermi level lies about 0.5–1 eV lower, giving an overall barrier between 3 and 5 eV in STM.

[14]T. Jung, F. J. Himpsel, R. Schlittler, and J. K. Gimzewski, in *STM IV-Analytical SXM Techniques*, edited by R. Wiesendanger, Springer Series in Surface Science (Springer, Berlin, 1998), Chap. 2, p. 11; T. Jung, Y. W. Mo, and F. J. Himpsel, Phys. Rev. Lett. **74**, 1641 (1995); F. J. Himpsel, T. Jung, R. Schlittler, and J. K. Gimzewski, Jpn. J. Appl. Phys., Part 1 **35**, 3695 (1996).

[15]J. Viernow, D. Y. Petrovykh, A. Kirakosian, J.-L. Lin, F. K. Men, M. Henzler, and F. J. Himpsel, Phys. Rev. B **59**, 10356 (1999).

[16]Y. A. Mo, J. Kleiner, M. B. Webb, and M. G. Lagally, Phys. Rev. Lett. **66**, 1998 (1991); J. A. Venables, Surf. Sci. **299/300**, 798 (1994).

[17]The temperature was determined by a Minolta–Land Cyclops 52 optical pyrometer with the emissivity set to 0.4 (estimated accuracy ±30°). The growth rate was typically 0.1 Å/s.

[18]A. M. Li, F. Liu, and M. G. Lagally, Bull. Am. Phys. Soc. **44**, 1714 (1999).

[19]A. B. Krasilnikov, A. V. Latyshev, and A. L. Aseev, Surf. Sci. **290**, 232 (1993); G. C. L. Wong, C. A. Lucas, D. Loretto, A. P. Payne, and P. H. Fuoss, Phys. Rev. Lett. **73**, 991 (1994); M. A. Olmstead, in *Heteroepitaxial Systems*, edited by A. W. K. Liu and M. Santos (World Scientific, Singapore, 1998), Chap. 5.

[20]J. Viernow, D. Y. Petrovykh, F. K. Men, A. Kirakosian, J.-L. Lin, and F. J. Himpsel, Appl. Phys. Lett. **74**, 2125 (1999).

[21]H. Rauscher, T. A. Jung, J.-L. Lin, A. Kirakosian, and F. J. Himpsel, Chem. Phys. Lett. **303**, 363 (1999).

[22]T. Jung, R. Schlittler, J. K. Gimzewski, and F. J. Himpsel, Appl. Phys. A: Mater. Sci. Process. **61**, 467 (1995).

[23]E. D. Williams and N. C. Bartelt, Science **251**, 393 (1991); J.Viernow, J.-L. Lin, D. Y. Petrovykh, F. M. Leibsle, F. K. Men, and F. J. Himpsel, Appl. Phys. Lett. **72**, 948 (1998).